HHS Public Access

Author manuscript

Cell Rep. Author manuscript; available in PMC 2020 November 23.

Published in final edited form as:

Cell Rep. 2020 October 20; 33(3): 108275. doi:10.1016/j.celrep.2020.108275.

TNF Receptor 1 Promotes Early-Life Immunity and Protects against Colitis in Mice

Cambrian Y. Liu[#1,6], **Sharon S. Tam**[#1,6], **Ying Huang**[#1,6], **Philip E. Dubé**[1], **Rabea Alhosh**[1], **Nandini Girish**[1], **Shivesh Punit**[1], **Shirin Nataneli**[1], **Fan Li**[2], **Jeffrey M. Bender**[2], **M. Kay Washington**[3], **D. Brent Polk**[1,4,5,7,*]

[1]Division of Pediatric Gastroenterology and Nutrition, The Saban Research Institute, Children's Hospital Los Angeles, Los Angeles, CA, USA

[2]Division of Infectious Diseases, Children's Hospital Los Angeles, Los Angeles, CA, USA

[3]Department of Pathology, Vanderbilt University Medical Center, Nashville, TN, USA

[4]Department of Pediatrics, Keck School of Medicine of the University of Southern California, Los Angeles, CA, USA

[5]Department of Biochemistry and Molecular Medicine, Keck School of Medicine of the University of Southern California, Los Angeles, CA, USA

[6]These authors contributed equally

[7]Lead Contact

[#] These authors contributed equally to this work.

SUMMARY

Neutralization of tumor necrosis factor (TNF) represents a widely used therapeutic strategy for autoimmune diseases including inflammatory bowel disease (IBD). However, the fact that many patients with IBD are non-responsive to anti-TNF therapies suggests the need for a better understanding of TNF signaling in IBD. Here, we show that co-deletion of TNF receptor 1 (TNFR1, *Tnfrsf1a*) in the *Il10*$^{-/-}$ spontaneous colitis model exacerbates disease, resulting in very-early-onset inflammation after weaning. The disease can be interrupted by treatment with antibiotics. The single deletion of TNFR1 induces subclinical colonic epithelial dysfunction and mucosal immune abnormalities, including accumulation of neutrophils and depletion of B cells. During the pre-disease period (before weaning), both *Tnfr1*$^{-/-}$ and *Il10*$^{-/-}$ *Tnfr1*$^{-/-}$ animals exhibit impaired expression of pro-inflammatory cytokines compared with wild-type and *Il10*$^{-/-}$

*Correspondence: dbpolk@chla.usc.edu.

AUTHOR CONTRIBUTIONS

C.Y.L., S.S.T., Y.H., P.E.D., and D.B.P. designed the study. Data acquisition and analysis were performed by C.Y.L., S.S.T., Y.H., R.A., S.P., N.G., S.N., and P.E.D. Sequencing data were analyzed by F.L., J.M.B., and C.Y.L. C.Y.L., S.S.T., Y.H., P.E.D., M.K.W., and D.B.P. interpreted the data. C.Y.L. wrote the manuscript. C.Y.L. and D.B.P. edited the manuscript.

SUPPLEMENTAL INFORMATION

Supplemental Information can be found online at https://doi.org/10.1016/j.celrep.2020.108275.

DECLARATION OF INTERESTS

The authors declare no competing interests.

controls, respectively. Collectively, these results demonstrate the net anti-inflammatory functions of TNF/TNFR1 signaling through the regulation of colonic immune homeostasis in early life.

Graphical Abstract

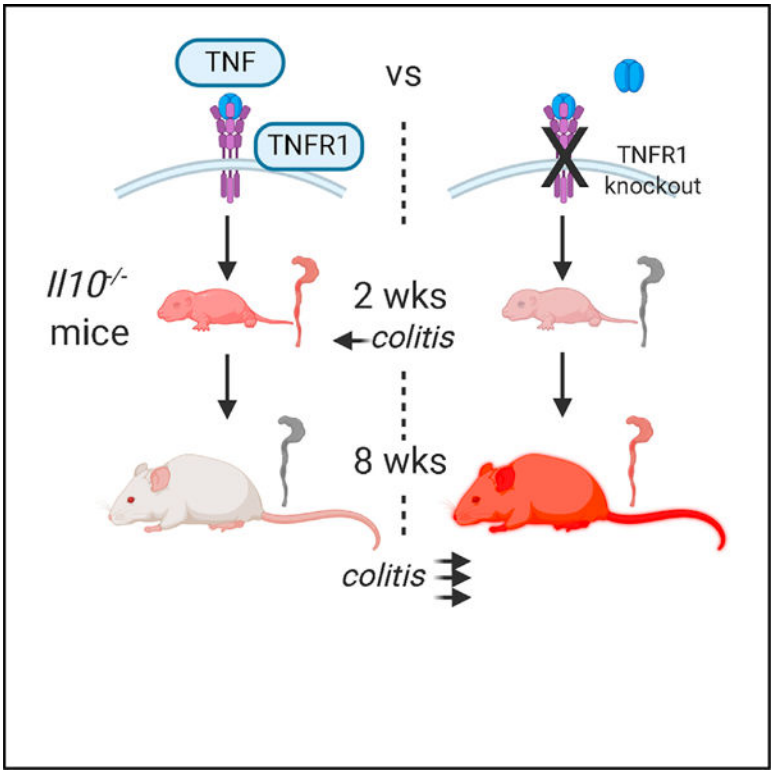

In Brief

Although anti-TNF therapies are used to treat colitis, Liu et al. demonstrate that colitis-susceptible mice deficient for TNF receptor 1 (TNFR1) paradoxically develop severe disease shortly after weaning. TNFR1 function can be traced back to its mediation of pro-inflammatory responses during a critical period of immune development in early life.

INTRODUCTION

The global incidence of inflammatory bowel disease (IBD) has increased steadily, especially in children under the age of 10 years (Benchimol et al., 2014; Kappelman et al., 2013; Schildkraut et al., 2013). A combination of host genetics, environmental exposures, intestinal mucosal dysfunction, and microbial dysbiosis contributes to IBD pathogenesis (Jostins et al., 2012). Although diverse genes and pathways regulate IBD susceptibility, their roles in immune development in early life and the biological mechanisms linking them to intestinal inflammation remain to be elucidated.

Tumor necrosis factor (TNF, formerly known as TNF-α) is a major therapeutic target in IBD. Pediatric patients with IBD have elevated circulating and intestinal levels of TNF (Breese et al., 1994; Murch et al., 1991). Recent genome-wide association studies (GWAS)

have identified mutations in the TNF signaling pathway to confer risk for both ulcerative colitis and Crohn's disease (Bank et al., 2014; Ferguson et al., 2009; Lappalainen et al., 2008; Li et al., 2016; McGovern et al., 2015; Pierik et al., 2004; Sashio et al., 2002; Waschke et al., 2005). The immediate therapeutic benefits of anti-TNF agents have suggested that TNF is a pro-inflammatory cytokine responsible for mucosal damage in IBD. However, the therapeutic effects of anti-TNF agents are short lived for many (Ben-Horin et al., 2014; Colombel et al., 2007; Ford et al., 2011; Schreiber et al., 2007). In mice, deletion of TNF or either of its transmembrane receptors, TNFR1 (p55) and TNFR2 (p75) (encoded by the *Tnfrsf1a* and *Tnfrsf1b* genes, respectively), has differing effects on disease susceptibility in established colitis models (Dubé et al., 2015; Ebach et al., 2005; Mizoguchi et al., 2008; Wang et al., 2012; Wang et al., 2013). Strikingly, loss of TNF-signaling-pathway members *Tnf* (Hale and Greer, 2012) or *Tnfr2* (Punit et al., 2015) results in severe disease in the *Il10*$^{-/-}$ spontaneous colitis model (Kühn et al., 1993). By ablating a critical tolerogenic signal, interleukin 10 (IL-10), the *Il10*$^{-/-}$ model replicates key features of Crohn's colitis, including the developmental dynamics of disease. However, the role of TNFR1 in the susceptibility to *Il10*$^{-/-}$ colitis has not, to our knowledge, been elucidated. It is not known whether TNFR1, on balance, would mediate the beneficial or deleterious effects of TNF signaling.

Here, we report severe, very-early-onset (VEO) colitis in *Il10*$^{-/-}$ *Tnfr1*$^{-/-}$ mice. Paradoxically, the early disease onset was preceded by impaired expression of pro-inflammatory cytokines during the period of life before weaning. TNFR1-mediated signaling in early life is, therefore, essential for the acquisition of mucosal tolerance.

RESULTS

Very-Early-Onset Colitis in *Il10*$^{-/-}$ *Tnfr1*$^{-/-}$ Mice

To characterize the role of TNFR1 in an animal model of spontaneous colitis, we bred *Tnfr1*$^{-/-}$ mice (Pfeffer et al., 1993) to *Il10*$^{-/-}$ mice (Kühn et al., 1993) to generate double-knockout animals. Consistent with previous reports (Bristol et al., 2000; Farmer et al., 2001; Mähler et al., 2002), Bl/6 *Il10*$^{-/-}$ mice are relatively resistant to colitis. *Il10*$^{-/-}$ *Tnfr1*$^{-/-}$ mice, however, developed severe, spontaneous, early-onset colitis, with a mixed mucosal infiltrate, cryptitis, abscesses, and epithelial hyperplasia. Although *Il10*$^{-/-}$ *Tnfr1*$^{-/-}$ animals at 2 (n = 8; Figures 1A and 1B) and 3 (n = 4, not shown) weeks old were spared colitis, whereas, at 4 weeks old, 8/13 (62%) of the *Il10*$^{-/-}$ *Tnfr1*$^{-/-}$ mice had histologic evidence of colitis (Figures 1C and 1D) (median histologic disease score: 7/15). At 6 weeks old, 4/7 (57%) of the *Il10*$^{-/-}$ *Tnfr1*$^{-/-}$ mice were colitic, and by 8 weeks old, 11/12 (92%) of the *Il10*$^{-/-}$ *Tnfr1*$^{-/-}$ mice had colitis (median histologic disease score: 8/15). Littermate *Il10*$^{-/-}$ mice had minimal disease (Figure 1E); moreover, heterozygous *Il10*$^{-/-}$ *Tnfr1*$^{+/-}$ littermates were spared severe disease and early mortality. Only 50% of *Il10*$^{-/-}$ *Tnfr1*$^{-/-}$ mice survived to 12 weeks old (Figures 1F, S1A, and S1B); their colons demonstrated increased RNA expression of cytokines, including *Tnf* (Figure 1G, from the NanoString assay) and increased crypt cell proliferation (phosphorylated histone H3 [pH-H3^{+}] cells; Figure 1H) and apoptosis (TUNEL^{+} cells; Figure 1I). The disease affected the entire colon and cecum, resulting in serrated adenocarcinoma (Figure S1C), and retarded growth in both males and

females (Figure S1D). This disease is, therefore, different from colitis in *Il10*$^{-/-}$ *Tnfr2*$^{-/-}$ mice, in which the cecum was not involved (Punit et al., 2015).

Because TNF signaling has integral roles in immune cell activation and specialization, we hypothesized that the loss of TNFR1 altered the relative proportions of the immune cells in colitis. We analyzed distal colonic mucosal scrapings by flow cytometry with a panel of 13 immune-cell-targeted antibodies (Figure S2) (Yu et al., 2016). Adult (8-week-old) *Il10*$^{-/-}$ *Tnfr1*$^{-/-}$ specimens showed elevated numbers of CD45^{+} (hematopoietic origin) cells compared with age- and litter-matched *Il10*$^{-/-}$ mice (Figure 1J), suggestive of increased immune cell infiltration into the mucosa. Within the CD45^{+} cell population, the relative proportions of neutrophils and activated CD4^{+} T cells were increased compared with those of the controls. However, several cell types showed a proportional reduction in the *Il10*$^{-/-}$ *Tnfr1*$^{-/-}$animals: B cells, intraepithelial lymphocytes, dendritic cells, and macrophages (Figure 1K). Thus, the loss of TNFR1 results in a fundamental imbalance of immune cell subtypes in the context of inflammation.

To determine whether TNFR1 expression protected from colitis in a general setting of IL-10 signaling inhibition, we assessed the susceptibility of *Tnfr1*$^{-/-}$ mice to colitis induced by repetitive administration of anti-IL-10 receptor-targeted antibodies (Figure S3A) (Carvalho et al., 2012; Kullberg et al., 2006; Singh et al., 2016). Antibody-injected *Tnfr1*$^{-/-}$ (knockout) mice exhibited crypt loss and mucosal immune infiltration, hallmarks of colitis, whereas antibody-injected *Tnfr1*$^{+/-}$ (heterozygous) mice were relatively protected from colitis (Figure S3B), as assessed histologically (Figure S3C). Thus, TNFR1 restricts colitis associated with the loss of IL-10 signaling.

Antibiotics Induce Remission of Colitis

Because IBD is thought to represent an abnormal immune reaction against gastrointestinal commensals, we tested whether antibiotics would alter the severe colonic injury observed in *Il10*$^{-/-}$ *Tnfr1*$^{-/-}$ mice. We treated 8-week-old *Il10*$^{-/-}$ *Tnfr1*$^{-/-}$ mice with neomycin and metronidazole for 2 weeks. Distal colonoscopy performed before and immediately after treatment showed resolution of the disease in the antibiotic-treated group (Figure 2A) compared with the vehicle-treated controls ($p = 0.0043$; Figure 2B). The difference in outcomes was apparent histologically ($p = 0.0042$; Figures 2C and 2D) and was associated with reduced numbers of pH-H3^{+} (proliferative) and cleaved caspase-3^{+} (apoptotic) cells (Figure 2E). In a mixed cohort of adult *Il10*$^{-/-}$ ($n = 7$) and *Il10*$^{-/-}$ *Tnfr1*$^{-/-}$ ($n = 2$) mice, we found that antibiotic treatment reduced fecal lipocalin, a marker of neutrophil activity, to baseline uninflamed levels (<50 pg/mg stool) within the first week of treatment (Figure 2F). Lipocalin levels rebounded within 1 week after antibiotic withdrawal. We noted diarrhea in *Il10*$^{-/-}$ *Tnfr1*$^{-/-}$ mice, which precluded the comparison of absolute lipocalin levels between genotypes. Taken together, these results indicate that disease continuation in *Il10*$^{-/-}$ *Tnfr1*$^{-/-}$ mice requires neomycin/metronidazole-sensitive commensals and that colonic epithelial and neutrophil abnormalities in these mice result from host-microbe interactions.

We next assessed whether the very-early-onset colitis observed in *Il10*$^{-/-}$ *Tnfr1*$^{-/-}$ mice was due to a distinct microbial ecosystem in early life. Using 16S sequencing, we profiled the luminal bacterial composition from the previously presented (Figure 1) cohort of littermate

Il10$^{-/-}$ and *Il10*$^{-/-}$ *Tnfr1*$^{-/-}$ mice at different ages. Analysis of variance (permutational multivariate analysis of variance [PERMANOVA]) showed that microbial composition was significantly associated with age ($p = 0.001$) and dam ($p = 0.01$) but not genotype ($p = 0.22$) (Figure 2G). The abundances of few operational taxonomic units (OTUs) were significantly altered at 2 weeks old, but alterations increased after onset of colitis at 4 weeks old (Figure 2H). We note that at 2 weeks old, low-abundance *Coriobacteriaceae* were depleted in *Il10*$^{-/-}$ *Tnfr1*$^{-/-}$ samples (Figure 2I), consistent with this taxon's reduced representation in pediatric IBD (Maukonen et al., 2015). At 8 weeks old, a qualitative difference in microbiome composition was observed (Figure 2G), but that difference was likely secondary to colitis. Colitic mice were depleted of *Lachnospiraceae*, a known producer of butyrate (Figure 2I) (Geirnaert et al., 2017; Surana and Kasper, 2017; Vital et al., 2014). Thus, a specific commensal signature did not cause exacerbated disease.

We next tested whether treatment of mice with antibiotics during the perinatal period would affect the onset of disease. Pregnant *Il10*$^{-/-}$ *Tnfr1*$^{+/-}$ dams were exposed to neomycin and metronidazole in their final week of pregnancy and up to 7 d postpartum. After treatment, F1 pups of all genotypes (*Il10*$^{-/-}$, *Il10*$^{-/-}$ *Tnfr1*$^{+/-}$, and *Il10*$^{-/-}$ *Tnfr1*$^{-/-}$) remained free of disease to at least 16 weeks old (Figure 2J). Heterozygous *Il10*$^{-/-}$ *Tnfr1*$^{+/-}$ pups were subsequently interbred, and their F2 pups of the *Il10*$^{-/-}$ *Tnfr1*$^{-/-}$ genotype exhibited colitis at 16 weeks old. Thus, the early onset of colitis in *Il10*$^{-/-}$ *Tnfr1*$^{-/-}$ mice can be interrupted by maternal treatment with antibiotics.

Colonic Mucosal Dysfunction in *Tnfr1*$^{-/-}$ Mice

To determine the specific contribution of TNFR1 to the colitic disease process, we analyzed the physiological effects of TNFR1 genetic loss in isolation, using *Il10*$^{+/+}$ *Tnfr1*$^{-/-}$ mice (or simply *Tnfr1*$^{-/-}$ mice). The fecal lipocalin levels of *Tnfr1*$^{-/-}$ mice at 12 weeks old were all <50 pg/mg stool ($n = 7$), suggesting that these mice did not have overt colitis. However, we found crypt fission, dropout, and branching (Figure 3A) in foci in 3/7 (43%) *Tnfr1*$^{-/-}$ mice. Moreover, at 4, 8, and 16 weeks old, *Tnfr1*$^{-/-}$ mice had significantly increased serum recovery of enemaadministered fluorescein isothiocyanate (FITC)-dextran (Figure 3B). *Tnfr1*$^{-/-}$ colonic crypts at 4 and 12 weeks old exhibited modestly elevated numbers of proliferating pH-H3^{+} cells (Figure 3C), and crypt abnormalities could also be identified in 4-week-old mice (Figure 3D; in 4/8 mice). At 12 weeks old, *Tnfr1*$^{-/-}$ mice had significantly ($p = 0.03$) increased numbers of DNA-damaged phosphorylated histone 2A.X (pH2A.X)-positive epithelial cells and phosphorylated STAT3-positive epithelial cells (Figure 3E). In contrast to *Il10*$^{-/-}$ *Tnfr1*$^{-/-}$ mice, intra-crypt staining for cleaved caspase-3 apoptotic bodies was not observed in *Tnfr1*$^{-/-}$ mice (not shown). TNFR1, therefore, regulates colonic epithelial function (e.g., morphology, permeability, and DNA-damage signaling) and repair (e.g., proliferation and STAT signaling) from a young age.

We also found significant immune defects through flow cytometry. There was a trending reduction ($p = 0.07$) in the total number of mucosal immune cells in 8-week-old *Tnfr1*$^{-/-}$ mice (Figure 3F). Although the proportions of T cells were similar between *Tnfr1*$^{-/-}$ and wild-type mice, the *Tnfr1*$^{-/-}$ mice showed an ~90% loss of B cells, consistent with prior reports of the TNFR1 role in the establishment of germinal centers (Le Hir et al., 1996;

Matsumoto et al., 1996; Pasparakis et al., 1996). Knockout mice showed a higher percentage of neutrophils (Figure 3G). Treatment of adult *Tnfr1*$^{-/-}$ mice with neomycin and metronidazole antibiotics for 2 weeks reduced the total representation of CD45^{+} hematopoietic cells, neutrophils (CD45^{+} Ly6G^{+}), and macrophages (CD45^{+} SSC^{hi} CD11b/c^{+} IA/IE^{+} CD24^{-}) (Figure 3H). However, antibiotic-driven reductions in colonic epithelial pH-H3 staining did not reach significance (Figure 3I). A reduced inter-crypt cellularity was histologically apparent in antibiotic-treated animals (Figure 3J). Thus, live commensals contribute to the mucosal defects associated with the loss of TNFR1.

Loss of TNFR1 Reduces Early-Life Cytokine Expression

The very-early onset of disease in *Il10*$^{-/-}$ *Tnfr1*$^{-/-}$ mice occurs shortly after the completion of the weaning process. We ordinarily separate pups from the dam at 3 weeks of age. Delaying that separation by 1 week (from 3 weeks old to 4 weeks old) did not prevent disease onset at 4 weeks (data not shown). Thus, the cause of disease cannot be reduced to this single ‘‘trigger’’ of maternal separation.

We next asked whether the effects of TNFR1 loss could be discerned in the pre-disease, early-life period. By high-throughput expression profiling, we examined the full-thickness colons of wild-type, *Tnfr1*$^{-/-}$, *Il10*$^{-/-}$, and *Il10*$^{-/-}$ *Tnfr1*$^{-/-}$ mice at ages corresponding to the pre-colitic (2 weeks) and colitic (8 weeks) states. In RNA sequencing (RNA-seq) studies comparing *Il10*$^{-/-}$ *Tnfr1*$^{-/-}$ and *Il10*$^{-/-}$ mice at 2 weeks old, we observed a profound downregulation of classical inflammatory markers, including *Nos2*, *Cxcl1*, *Saa1*, and calprotectin (*S100a8* and *S100a9*), in the double-knockout mice (Figure 4A). We analyzed those cytokines as a group, the ‘‘TNFR1-associated early-life immune module,’’ and calculated a score (-1.7 ± 0.35, their mean logarithmic expression ratio between TNFR1-deficient and TNFR1-expressing conditions), which quantified their overall change (Figure 4B). That score was significantly less than zero ($p = 3 \times 10^{-5}$), supporting the overall reduced expression of those cytokines in *Il10*$^{-/-}$ *Tnfr1*$^{-/-}$ mice at 2 weeks of age. At 8 weeks old, these immune markers had a positive ($p = 0.003$) expression score of 3.4 ± 1.0 in *Il10*$^{-/-}$ *Tnfr1*$^{-/-}$ (versus age-matched *Il10*$^{-/-}$) animals, consistent with their broad upregulation in colitis. This pattern of changes was preserved in *Tnfr1*$^{-/-}$ mice that had genetically functional IL-10, although the magnitude of the changes was less. Adult *Tnfr1*$^{-/-}$ mice had elevated expression of neutrophil-associated genes, such as the calprotectin subunits (*S100a8*, *S100a9*) and *Duox2*. In contrast, pre-weaning *Tnfr1*$^{-/-}$ mice at 2 weeks old exhibited reduced transcription of *Il1b* (IL-1b) (Figure 4A). qPCR studies showed that adult heterozygous *Tnfr1*$^{+/-}$ mice had similar calprotectin expression as wild-type littermates (Figure S4A).

Cytokine changes were associated with functional defects. There was more epithelial pH-H3 (proliferative) staining in 2-week-old *Il10*$^{-/-}$ colons versus *Il10*$^{-/-}$ *Tnfr1*$^{-/-}$ colons (Figure 4C), in marked contrast to results in 8-week-old mice (Figure 1H). On flow-cytometric analysis, we found similar proportions of CD45^{+} cells (Figure 4D) and neutrophils (Figure 4E) in 2-week-old animals across all genotypes. However, reduction in B cell numbers in TNFR1-deficient animals was already evident at 2 weeks of age (Figure 4E). Thus, loss of TNFR1 results in profound immune and epithelial defects in early life.

We ruled out that transcriptional changes in *Tnfr1*$^{-/-}$ mice were compensated for by TNFR2. We compared transcriptomic profiles of adult *Tnfr1*$^{-/-}$ mice and *Tnfr2*$^{-/-}$ mice (Punit et al., 2015). As shown in Figure S4B, there was little overlap (4%) of differentially expressed transcripts in *Tnfr1*$^{-/-}$ and *Tnfr2*$^{-/-}$ colons. Among the few co-regulated transcripts, there was a significant negative correlation in their direction of regulation (Figure S4C). The loss of *Tnfr1* did not affect expression of *Tnfr2* and vice versa. Notably, *Saa2* and *Duox2*, associated with abnormal mucosal immune responses to microbiota (Eckhardt et al., 2010; Grasberger et al., 2015), were both upregulated in the absence of either TNFR1 or TNFR2.

DISCUSSION

Here, we show that the genetic loss of TNFR1 results in increased susceptibility to colitis. The early age of disease onset in *Il10*$^{-/-}$ *Tnfr1*$^{-/-}$ mice, after weaning, may be functionally equivalent to infantile or toddler colitis in humans (assuming full weaning at 1–2 years of age). In rodents, at that age, the colonic mucosa undergoes histological maturation (Walthall et al., 2005). During the simultaneous immune ‘‘weaning reaction,’’ pro-inflammatory signals act against intestinal luminal contents to ultimately promote tolerance through the establishment of immunosuppressive cell populations (Al Nabhani et al., 2019; Olszak et al., 2012; Pié et al., 2004; Redhu et al., 2017; Scheer et al., 2017). The results of our study can be interpreted within that framework and demonstrate that TNFR1-mediated pro-inflammatory signaling, including upregulation of *Il1b*, in early life is essential for the weaning reaction (Pié et al., 2004). These results demonstrate how immunodeficiency during early life can predispose animals toward later autoimmunity, as hinted at by studies of other genetic immunodeficiencies (Glocker and Grimbacher, 2012; Mombaerts et al., 1993; Sadlack et al., 1993; Salzer et al., 2014; Tegtmeyer et al., 2017).

The exacerbation of colitis with TNFR1 loss in mice could partially model the uneven clinical efficacy of anti-TNF antibodies in IBD (Gratz et al., 2002; Kullberg et al., 2001; Scheinin et al., 2003), increased risk for human IBD associated with genetic perturbation of TNF receptors, and new-onset IBD in autoimmune patients treated with anti-TNF (Korzenik et al., 2019; Toussirot et al., 2012; Üsküdar Cansu et al., 2019). Relevant to this study, very-early-onset IBD is frequently linked to the loss of the IL-10 receptor (Bianco et al., 2015) (Begue et al., 2011; Beser et al., 2015; Kotlarz et al., 2012; Moran et al., 2013; Pigneur et al., 2013). Elucidating key functions in TNF receptor signaling in intestinal development and inflammation may have therapeutic benefits.

Limitations of Study

First, it is premature to generalize our findings directly to human anti-TNF therapies, which may work through distinct mechanisms (e.g., Atreya et al., 2011). Second, we have had only limited success in pharmacological manipulation of the weaning reaction in colitis. Third, we do not know whether immune cell alterations and epithelial dysfunction in *Tnfr1*$^{-/-}$ animals are caused by one or the other. Future studies will need to elaborate on these aspects of TNF signaling in colitis.

STAR★METHODS

RESOURCE AVAILABILITY

Lead Contact—Further information and requests for resources and reagents should be directed to and will be fulfilled by the Lead Contact, Brent Polk (dbpolk@chla.usc.edu).

Materials Availability—This study did not generate new unique reagents.

Data and Code Availability—The RNA-seq datasets generated during this study are available at NCBI Gene Expression Omnibus (accession numbers): GSE107933, GSE155654, GSE155626).

EXPERIMENTAL MODEL AND SUBJECT DETAILS

Mice—Mice were maintained humanely, in accordance with the rules and regulations of the Institutional Animal Care and Use Committee (IACUC) of Children's Hospital Los Angeles (CHLA). This study was approved by the CHLA IACUC under the internal protocol number 288. Mice were anesthetized with isoflurane and euthanized via cervical dislocation prior to dissection.

Wild-type (WT), *Il10*$^{-/-}$ (stock #002251), and *Tnfr1*$^{-/-}$(stock #002818) mice on the C57BL/6J background were obtained from Jackson Laboratory. *Il10*$^{-/-}$ *Tnfr1*$^{-/-}$ mice and control *Il10*$^{-/-}$ littermates were generated from *Il10*$^{-/-}$ *Tnfr1*$^{+/-}$ parents. Experimental and control groups of mice were co-housed for > 4 weeks prior to experimentation, and co-housing was maintained during experimentation. Both male and female mice were included in the study. Details regarding the ages of mice used in experiments are given in the description of Results.

METHOD DETAILS

Tissue collection—Colons and ceca were carefully freed from the abdominal cavity of euthanized mice, opened longitudinally, and cleaned of fecal contents. Luminal contents of the ceca were collected for bacterial 16S rRNA sequencing. Colons were opened and splayed; a thin longitudinal strip representing the full proximal-distal length of each colon was removed and preserved for RNA isolation. The remaining tissue was fixed overnight in 10% neutral buffered formalin at room temperature. For histological assessment, colons were washed with 50% ethanol, dehydrated in an ascending ethanol series, cleared with xylenes, and embedded in molten paraffin. Thin (5 μm) sections were prepared on a microtome and stored until their usage in staining procedures.

Histochemistry—Blinded to sample origin, assessment of colitis severity was made on hematoxylin and eosin-stained sections of murine colon by MKW using previously validated and published methodologies (Dubé et al., 2012; Zhang et al., 2012). Histology was scored based on 5 categories: enterocyte loss, crypt inflammation, lamina propria mononuclear cells, polymorphonuclear cells, and hyperplasia. Each category is awarded a score from 0 to 3, with higher score indicating more severe disease. A maximum score of 15 is assigned. For quantification of epithelial cell markers, label-positive cells in 30–100 crypts adjacent to the

anal verge were counted and divided by the total number of counted crypts to yield a per-crypt number.

Immunohistochemistry was performed using standard protocols. Primary antibodies were incubated at 4°C overnight. Primary antibodies used were rabbit anti-pH2A.X (Ser139) (Cell Signaling Technology #9718S, 1:2,000 dilution), rabbit anti-pHH3 (Ser10) (Cell Signaling Technology #9701S, 1:500 dilution), rabbit anti-pSTAT3 (Tyr705) (Cell Signaling Technology #9145, 1:100 dilution), and rabbit anti-cCSP3 (Cell Signaling Technology #9661S, 1:200 dilution).

Flow Cytometry—Colons were freshly dissected from mice. If the colon was isolated from an adult (8-wk-old) animal, the mucosal layer was separated from the muscle layer using fine forceps. The mucosal piece was minced into 2-mm^2 pieces. If the colon was isolated from an unweaned (2-wk-old) mouse, the full-thickness organ was immediately minced into 2-mm^2 pieces.

Tissue was incubated with prewarmed digestion solution (0.2 Wunsch units/ml Liberase TM + 200 Kuntz units/ml DNase I in DMEM/F12 + 15 mM HEPES) for 30 min at 37°C with continuous agitation at 180 rpm. After trituration of the tissue and its passage through a 70-μm-pore cell strainer, the tissue was washed with DMEM:F12 supplemented with 10% FBS, and then also with HEPES-buffered saline (Liu et al., 2012) supplemented with 0.5% BSA. All subsequent washes and stainings were performed in HBS+0.5% BSA. The tissue was stained with 0.1 μM DAPI, blocked for 15 min at 4°C with a solution composed of 5% mouse/rat serum supplemented with mouse Fc block (anti-CD16/32 antibody, Biolegend ‘‘truStain fx’’), and probed with a mixture of preconjugated antibodies for 30 min at 4°C. Antibodies (working dilutions) were targeted to CD45 (1:250), Ly6G (1:200), CD11b (1:200), CD11c (1:100), IA/IE (1:1,000), CD64 (1:400), CD24 (1:500), Ly6C (1:200), CD69 (1:200), CD8 (1:100), CD4 (1:200), TCRd (1:200), and CD3 (1:200). After washes, cells were analyzed on a BD LSR II. Compensation was adjusted using references obtained by the analysis of antibodies bound to Ultracomp eBeads (ThermoFisher Scientific).

Analysis of flow cytometric data was performed using FlowJo. Gates were adjusted for each experimental day but were consistent between experimental and control samples. Data were pooled across 3–4 experimental days per genotype/age comparison.

Collection and analysis of stool—Stool pellets were collected from mice by manual restraint which typically induced defecation within 30 s. A clean Eppendorf tube was held beneath the anal opening. Pellets were frozen at −80°C and analyzed for fecal lipocalin-2 levels using a commercial ELISA kit and according to the manufacturer’s instructions (R&D Systems, cat# DY1857).

Antibiotic treatment—*Il10*$^{-/-}$ *Tnfr1*$^{-/-}$ mice at 8 weeks of age were assigned to either ‘Vehicle’ or ‘Antibiotics’ treatment group (n = 3 in each group). Mice received either water (‘Vehicle’) or broad-spectrum antibiotics for 2 weeks (Neomycin sulfate 500mg tablets purchased from Hi-Tech Pharmacal, Metronidazole 500mg/100ml purchased from Claris Lifescience) *ad libitum*. Both antibiotics were mixed with drinking water at 1 g/L. Distal

colonoscopy on deeply anesthetized mice was performed pre- and post-treatment using a flexible instrument (Karl Storz). Mice were euthanized post-treatment at 10 weeks of age, and colon histology was scored as previously described (Dubé et al., 2012; Punit et al., 2015) to determine colitis severity.

16S sequencing—16S rRNA libraries were prepared from flash-frozen cecal contents. Cecal content was collected from co-housed littermates of *Il10*$^{-/-}$ and *Il10*$^{-/-}$ *Tnfr1*$^{-/-}$ mice euthanized at 2, 4, 6, and 8 weeks. Cecal content was frozen immediately after collection and stored at −80°C. Cecal microbiome composition was determined by sequencing the 16S ribosomal RNA gene. Sequencing was performed on the Illumina MiSeq platform (Diversity assay 2x300bp 20K bTEFAP® at *MR DNA* lab (Shallowater, TX USA)).

Expression analysis of immune-related transcripts—RNA was extracted from colon tissues using standard RNA extraction techniques (PureLink® RNA Mini Kit from Ambion) and assayed for mRNA expression of targeted immune genes using the Nanostring technology (nCounter Mouse Immunology Panel, 561 genes).

RNA-Seq—mRNA transcripts were purified from total colonic RNA using oligo-dT coated beads, sheared, and prepared for 2x75 bp sequencing on a HiSeq 4000 (Illumina). Library preparation and sequencing were performed by SeqMatic, LLC (Fremont, CA USA).

Barrier function assay—WT and *Tnfr1*$^{-/-}$ mice were co-housed for minimum of 1-week prior to experiment. Mice were sedated and a 0.2 mL volume of fluorescein (FITC)-dextran (MW 3000, Invitrogen, 50 mg/ml solution in PBS) was instilled into the rectum with a 3.5 Fr catheter. Blood was obtained 30 minutes later through a retro-orbital blood draw. Plasma fluorescence was measured in a plate reader (excitation 490nm; emission 520nm).

Anti-IL10R model of colitis—Co-housed *Tnfr1*$^{+/-}$ and *Tnfr1*$^{-/-}$ mice were intraperitoneally injected, on alternating sides of body, with 1 mg/mouse/dose of anti-IL10R antibody once per week, for a total of 3 injections. Injections were begun when mice were 3 wks old. Euthanasia and postmortem analyses were performed at 6 wks of age.

QUANTIFICATION AND STATISTICAL ANALYSIS

Gene abundance estimates—Transcript quantification and significance testing from RNA-Seq data were performed using the paired-end read option on kallisto/sleuth (Bray et al., 2016). Differential expression of expression data obtained using the Nanostring platform was computed using nSolver version 3.0 software (Nanostring).

Operational taxonomic units (OTUs) were generated from 16S sequences by clustering at 3% divergence (97% similarity) in mothur (Schloss et al., 2009). Final OTUs were taxonomically classified against a curated database derived from the Ribosomal Database Project (Cole et al., 2014) and NCBI. Additional analyses were performed using the ‘phyloseq’ (v1.19.1) (McMurdie and Holmes, 2013) and ‘vegan’ (v2.4–2) (Dixon, 2003) packages in R (version 3.3). Random forest regression was used to predict colitis score with OTU relative abundances as covariates (‘randomForest’ package v4.6). Only OTUs with > =

1% relative abundance in at least 5 samples were used. Linear discriminant analysis was performed using LEfSe (Segata et al., 2011).

Statistical tests—Data are presented as individual points with summary statistics reporting the mean and standard error of the mean. Significance was evaluated using the t test, unless otherwise noted.

Supplementary Material

Refer to Web version on PubMed Central for supplementary material.

ACKNOWLEDGMENTS

This study was supported by the U.S. National Institutes of Health (R01-DK056008 and R01-DK108648, to D.B.P.), the Crohn's and Colitis Foundation (career development award to C.Y.L., postdoctoral fellowship to P.E.D., and senior research award to D.B.P.), and the California Institute for Regenerative Medicine (postdoctoral fellowship to C.Y.L.). We would like to thank Tsen-Yin Lin, Michael Sheard, Elizabeth Lopez, Gricelda Vasquez, and Chris Escolano for technical advice and care of animals.

REFERENCES

Al Nabhani Z, Dulauroy S, Marques R, Cousu C, Al Bounny S, Dejardin F, Sparwasser T, Berard M, Cerf-Bensussan N, and Eberl G (2019). A weaning reaction to microbiota is required for resistance to immunopathologies in the adult. Immunity 50, 1276–1288.e1275. [PubMed: 30902637]

Atreya R, Zimmer M, Bartsch B, Waldner MJ, Atreya I, Neumann H, Hildner K, Hoffman A, Kiesslich R, Rink AD, et al. (2011). Antibodies against tumor necrosis factor (TNF) induce T-cell apoptosis in patients with inflammatory bowel diseases via TNF receptor 2 and intestinal $CD14^{+}$ macrophages. Gastroenterology 141, 2026–2038. [PubMed: 21875498]

Bank S, Skytt Andersen P, Burisch J, Pedersen N, Roug S, Galsgaard J, Ydegaard Turino S, Brodersen JB, Rashid S, Kaiser Rasmussen B, et al. (2014). Polymorphisms in the inflammatory pathway genes TLR2, TLR4, TLR9, LY96, NFKBIA, NFKB1, TNFA, TNFRSF1A, IL6R, IL10, IL23R, PTPN22, and PPARG are associated with susceptibility of inflammatory bowel disease in a Danish cohort. PLoS ONE 9, e98815. [PubMed: 24971461]

Begue B, Verdier J, Rieux-Laucat F, Goulet O, Morali A, Canioni D, Hugot JP, Daussy C, Verkarre V, Pigneur B, et al. (2011). Defective IL10 signaling defining a subgroup of patients with inflammatory bowel disease. Am. J. Gastroenterol 106, 1544–1555. [PubMed: 21519361]

Ben-Horin S, Kopylov U, and Chowers Y (2014). Optimizing anti-TNF treatments in inflammatory bowel disease. Autoimmun. Rev 13, 24–30. [PubMed: 23792214]

Benchimol EI, Manuel DG, Guttmann A, Nguyen GC, Mojaverian N, Quach P, and Mack DR (2014). Changing age demographics of inflammatory bowel disease in Ontario, Canada: a population-based cohort study of epidemiology trends. Inflamm. Bowel Dis 20, 1761–1769. [PubMed: 25159453]

Beser OF, Conde CD, Serwas NK, Cokugras FC, Kutlu T, Boztug K, and Erkan T (2015). Clinical features of interleukin 10 receptor gene mutations in children with very early-onset inflammatory bowel disease. J. Pediatr. Gastroenterol. Nutr 60, 332–338. [PubMed: 25373860]

Bianco AM, Girardelli M, and Tommasini A (2015). Genetics of inflammatory bowel disease from multifactorial to monogenic forms. World J. Gastroenterol 21, 12296–12310. [PubMed: 26604638]

Bray NL, Pimentel H, Melsted P, and Pachter L (2016). Near-optimal probabilistic RNA-seq quantification. Nat. Biotechnol 34, 525–527. [PubMed: 27043002]

Breese EJ, Michie CA, Nicholls SW, Murch SH, Williams CB, Domizio P, Walker-Smith JA, and MacDonald TT (1994). Tumor necrosis factor alpha-producing cells in the intestinal mucosa of children with inflammatory bowel disease. Gastroenterology 106, 1455–1466. [PubMed: 8194690]

Bristol IJ, Farmer MA, Cong Y, Zheng XX, Strom TB, Elson CO, Sundberg JP, and Leiter EH (2000). Heritable susceptibility for colitis in mice induced by IL-10 deficiency. Inflamm. Bowel Dis 6, 290–302. [PubMed: 11149562]

Carvalho FA, Nalbantoglu I, Ortega-Fernandez S, Aitken JD, Su Y, Koren O, Walters WA, Knight R, Ley RE, Vijay-Kumar M, and Gewirtz AT (2012). Interleukin-1b (IL-1b) promotes susceptibility of Toll-like receptor 5 (TLR5) deficient mice to colitis. Gut 61, 373–384. [PubMed: 21646247]

Cole JR, Wang Q, Fish JA, Chai B, McGarrell DM, Sun Y, Brown CT, Porras-Alfaro A, Kuske CR, and Tiedje JM (2014). Ribosomal Database Project: data and tools for high throughput rRNA analysis. Nucleic Acids Res 42, D633–D642. [PubMed: 24288368]

Colombel JF, Sandborn WJ, Rutgeerts P, Enns R, Hanauer SB, Panaccione R, Schreiber S, Byczkowski D, Li J, Kent JD, and Pollack PF (2007). Adalimumab for maintenance of clinical response and remission in patients with Crohn's disease: the CHARM trial. Gastroenterology 132, 52–65. [PubMed: 17241859]

Dixon P (2003). VEGAN, a package of R functions for community ecology. J. Veg. Sci 14, 927–930.

Dubé PE, Yan F, Punit S, Girish N, McElroy SJ, Washington MK, and Polk DB (2012). Epidermal growth factor receptor inhibits colitis-associated cancer in mice. J. Clin. Invest 122, 2780–2792. [PubMed: 22772467]

Dubé PE, Punit S, and Polk DB (2015). Redeeming an old foe: protective as well as pathophysiological roles for tumor necrosis factor in inflammatory bowel disease. Am. J. Physiol. Gastrointest. Liver Physiol 308, G161–G170. [PubMed: 25477373]

Ebach DR, Newberry R, and Stenson WF (2005). Differential role of tumor necrosis factor receptors in TNBS colitis. Inflamm. Bowel Dis 11, 533–540. [PubMed: 15905700]

Eckhardt ER, Witta J, Zhong J, Arsenescu R, Arsenescu V, Wang Y, Ghoshal S, de Beer MC, de Beer FC, and de Villiers WJ (2010). Intestinal epithelial serum amyloid A modulates bacterial growth in vitro and pro-inflammatory responses in mouse experimental colitis. BMC Gastroenterol 10, 133. [PubMed: 21067563]

Farmer MA, Sundberg JP, Bristol IJ, Churchill GA, Li R, Elson CO, and Leiter EH (2001). A major quantitative trait locus on chromosome 3 controls colitis severity in IL-10-deficient mice. Proc. Natl. Acad. Sci. USA 98, 13820–13825. [PubMed: 11707574]

Ferguson LR, Han DY, Huebner C, Petermann I, Barclay ML, Gearry RB, McCulloch A, and Demmers PS (2009). Tumor necrosis factor receptor superfamily, member 1B haplotypes increase or decrease the risk of inflammatory bowel diseases in a New Zealand caucasian population. Gastroenterol. Res. Pract 2009, 591704. [PubMed: 19421420]

Ford AC, Sandborn WJ, Khan KJ, Hanauer SB, Talley NJ, and Moayyedi P (2011). Efficacy of biological therapies in inflammatory bowel disease: systematic review and meta-analysis. Am. J. Gastroenterol 106, 644–659, quiz 660. [PubMed: 21407183]

Geirnaert A, Calatayud M, Grootaert C, Laukens D, Devriese S, Smagghe G, De Vos M, Boon N, and Van de Wiele T (2017). Butyrate-producing bacteria supplemented in vitro to Crohn's disease patient microbiota increased butyrate production and enhanced intestinal epithelial barrier integrity. Sci. Rep 7, 11450. [PubMed: 28904372]

Glocker E, and Grimbacher B (2012). Inflammatory bowel disease: is it a primary immunodeficiency? Cell. Mol. Life Sci 69, 41–48. [PubMed: 21997382]

Grasberger H, Gao J, Nagao-Kitamoto H, Kitamoto S, Zhang M, Kamada N, Eaton KA, El-Zaatari M, Shreiner AB, Merchant JL, et al. (2015). Increased expression of DUOX2 is an epithelial response to mucosal dysbiosis required for immune homeostasis in mouse intestine. Gastroenterology 149, 1849–1859. [PubMed: 26261005]

Gratz R, Becker S, Sokolowski N, Schumann M, Bass D, and Malnick SD (2002). Murine monoclonal anti-tNF antibody administration has a beneficial effect on inflammatory bowel disease that develops in IL-10 knockout mice. Dig. Dis. Sci 47, 1723–1727. [PubMed: 12184521]

Hale LP, and Greer PK (2012). A novel murine model of inflammatory bowel disease and inflammation-associated colon cancer with ulcerative colitis-like features. PLoS ONE 7, e41797. [PubMed: 22848611]

Jostins L, Ripke S, Weersma RK, Duerr RH, McGovern DP, Hui KY, Lee JC, Schumm LP, Sharma Y, Anderson CA, et al.; International IBD Genetics Consortium (IIBDGC) (2012). Host-microbe

interactions have shaped the genetic architecture of inflammatory bowel disease. Nature 491, 119–124. [PubMed: 23128233]

Kappelman MD, Moore KR, Allen JK, and Cook SF (2013). Recent trends in the prevalence of Crohn's disease and ulcerative colitis in a commercially insured US population. Dig. Dis. Sci 58, 519–525. [PubMed: 22926499]

Korzenik J, Larsen MD, Nielsen J, Kjeldsen J, and Nørgård BM (2019). Increased risk of developing Crohn's disease or ulcerative colitis in 17 018 patients while under treatment with anti-TNFa agents, particularly etanercept, for autoimmune diseases other than inflammatory bowel disease. Aliment. Pharmacol. Ther 50, 289–294. [PubMed: 31267570]

Kotlarz D, Beier R, Murugan D, Diestelhorst J, Jensen O, Boztug K, Pfeifer D, Kreipe H, Pfister ED, Baumann U, et al. (2012). Loss of interleukin-10 signaling and infantile inflammatory bowel disease: implications for diagnosis and therapy. Gastroenterology 143, 347–355. [PubMed: 22549091]

Kühn R, Löhler J, Rennick D, Rajewsky K, and Müller W (1993). Interleukin-10-deficient mice develop chronic enterocolitis. Cell 75, 263–274. [PubMed: 8402911]

Kullberg MC, Rothfuchs AG, Jankovic D, Caspar P, Wynn TA, Gorelick PL, Cheever AW, and Sher A (2001). Helicobacter hepaticus-induced colitis in interleukin-10-deficient mice: cytokine requirements for the induction and maintenance of intestinal inflammation. Infect. Immun 69, 4232–4241. [PubMed: 11401959]

Kullberg MC, Jankovic D, Feng CG, Hue S, Gorelick PL, McKenzie BS, Cua DJ, Powrie F, Cheever AW, Maloy KJ, and Sher A (2006). IL-23 plays a key role in Helicobacter hepaticus-induced T cell-dependent colitis. J. Exp. Med 203, 2485–2494. [PubMed: 17030948]

Lappalainen M, Halme L, Turunen U, Saavalainen P, Einarsdottir E, Färkkilä M, Kontula K, and Paavola-Sakki P (2008). Association of IL23R, TNFRSF1A, and HLA-DRB1*0103 allele variants with inflammatory bowel disease phenotypes in the Finnish population. Inflamm. Bowel Dis 14, 1118–1124. [PubMed: 18338763]

Le Hir M, Bluethmann H, Kosco-Vilbois MH, Müller M, di Padova F, Moore M, Ryffel B, and Eugster HP (1996). Differentiation of follicular dendritic cells and full antibody responses require tumor necrosis factor receptor-1 signaling. J. Exp. Med 183, 2367–2372. [PubMed: 8642347]

Li D, Silverberg MS, Haritunians T, Dubinsky MC, Landers C, Stempak JM, Milgrom R, Guo X, Chen YD, Rotter JI, et al. (2016). TNFRSF1B Is Associated with ANCA in IBD. Inflamm. Bowel Dis 22, 1346–1352. [PubMed: 27104820]

Liu CY, Xiao C, Fraser SE, Lester HA, and Koos DS (2012). Electrophysiological characterization of Grueneberg ganglion olfactory neurons: spontaneous firing, sodium conductance, and hyperpolarization-activated currents. J. Neurophysiol 108, 1318–1334. [PubMed: 22649209]

Mähler M, Most C, Schmidtke S, Sundberg JP, Li R, Hedrich HJ, and Churchill GA (2002). Genetics of colitis susceptibility in IL-10-deficient mice: backcross versus F2 results contrasted by principal component analysis. Genomics 80, 274–282. [PubMed: 12213197]

Matsumoto M, Mariathasan S, Nahm MH, Baranyay F, Peschon JJ, and Chaplin DD (1996). Role of lymphotoxin and the type I TNF receptor in the formation of germinal centers. Science 271, 1289–1291. [PubMed: 8638112]

Maukonen J, Kolho KL, Paasela M, Honkanen J, Klemetti P, Vaarala O, and Saarela M (2015). Altered fecal microbiota in paediatric inflammatory bowel disease. J. Crohn's Colitis 9, 1088–1095. [PubMed: 26351391]

McGovern DPB, Kugathasan S, and Cho JH (2015). Genetics of inflammatory bowel diseases. Gastroenterology 149, 1163–1176.e1162. [PubMed: 26255561]

McMurdie PJ, and Holmes S (2013). phyloseq: an R package for reproducible interactive analysis and graphics of microbiome census data. PLoS ONE 8, e61217. [PubMed: 23630581]

Mizoguchi E, Hachiya Y, Kawada M, Nagatani K, Ogawa A, Sugimoto K, Mizoguchi A, and Podolsky DK (2008). TNF receptor type I-dependent activation of innate responses to reduce intestinal damage-associated mortality. Gastroenterology 134, 470–480. [PubMed: 18242213]

Mombaerts P, Mizoguchi E, Grusby MJ, Glimcher LH, Bhan AK, and Tonegawa S (1993). Spontaneous development of inflammatory bowel disease in T cell receptor mutant mice. Cell 75, 274–282. [PubMed: 8104709]

Moran CJ, Walters TD, Guo CH, Kugathasan S, Klein C, Turner D, Wolters VM, Bandsma RH, Mouzaki M, Zachos M, et al. (2013). IL-10R polymorphisms are associated with very-early-onset ulcerative colitis. Inflamm. Bowel Dis 19, 115–123. [PubMed: 22550014]

Murch SH, Lamkin VA, Savage MO, Walker-Smith JA, and MacDonald TT (1991). Serum concentrations of tumour necrosis factor alpha in childhood chronic inflammatory bowel disease. Gut 32, 913–917. [PubMed: 1885073]

Olszak T, An D, Zeissig S, Vera MP, Richter J, Franke A, Glickman JN, Siebert R, Baron RM, Kasper DL, and Blumberg RS (2012). Microbial exposure during early life has persistent effects on natural killer T cell function. Science 336, 489–493. [PubMed: 22442383]

Pasparakis M, Alexopoulou L, Episkopou V, and Kollias G (1996). Immune and inflammatory responses in TNF alpha-deficient mice: a critical requirement for TNF alpha in the formation of primary B cell follicles, follicular dendritic cell networks and germinal centers, and in the maturation of the humoral immune response. J. Exp. Med 184, 1397–1411. [PubMed: 8879212]

Pfeffer K, Matsuyama T, Kündig TM, Wakeham A, Kishihara K, Shahinian A, Wiegmann K, Ohashi PS, Krönke M, and Mak TW (1993). Mice deficient for the 55 kd tumor necrosis factor receptor are resistant to endotoxic shock, yet succumb to L. monocytogenes infection. Cell 73, 457–467. [PubMed: 8387893]

Pié S, Lallès JP, Blazy F, Laffitte J, Sève B, and Oswald IP (2004). Weaning is associated with an upregulation of expression of inflammatory cytokines in the intestine of piglets. J. Nutr 134, 641–647. [PubMed: 14988461]

Pierik M, Vermeire S, Steen KV, Joossens S, Claessens G, Vlietinck R, and Rutgeerts P (2004). Tumour necrosis factor-alpha receptor 1 and 2 polymorphisms in inflammatory bowel disease and their association with response to infliximab. Aliment. Pharmacol. Ther 20, 303–310. [PubMed: 15274667]

Pigneur B, Escher J, Elawad M, Lima R, Buderus S, Kierkus J, Guariso G, Canioni D, Lambot K, Talbotec C, et al. (2013). Phenotypic characterization of very early-onset IBD due to mutations in the IL10, IL10 receptor alpha or beta gene: a survey of the Genius Working Group. Inflamm. Bowel Dis 19, 2820–2828. [PubMed: 24216686]

Punit S, Dube PE, Liu CY, Girish N, Washington MK, and Polk DB (2015). Tumor necrosis factor receptor 2 restricts the pathogenicity of $CD8^+$ T cells in mice with colitis. Gastroenterology 149, 993–1005.e1002. [PubMed: 26072395]

Redhu NS, Bakthavatchalu V, Conaway EA, Shouval DS, Tsou A, Goettel JA, Biswas A, Wang C, Field M, Muller W, et al. (2017). Macrophage dysfunction initiates colitis during weaning of infant mice lacking the interleukin-10 receptor. eLife 6, 6.

Sadlack B, Merz H, Schorle H, Schimpl A, Feller AC, and Horak I (1993). Ulcerative colitis-like disease in mice with a disrupted interleukin-2 gene. Cell 75, 253–261. [PubMed: 8402910]

Salzer E, Kansu A, Sic H, Majek P, Ikinciogullari A, Dogu FE, Prengemann NK, Santos-Valente E, Pickl WF, Bilic I, et al. (2014). Early-onset inflammatory bowel disease and common variable immunodeficiency-like disease caused by IL-21 deficiency. J. Allergy Clin. Immunol. 133, 1651–1659.e1612. [PubMed: 24746753]

Sashio H, Tamura K, Ito R, Yamamoto Y, Bamba H, Kosaka T, Fukui S, Sawada K, Fukuda Y, Tamura K, et al. (2002). Polymorphisms of the TNF gene and the TNF receptor superfamily member 1B gene are associated with susceptibility to ulcerative colitis and Crohn's disease, respectively. Immunogenetics 53, 1020–1027. [PubMed: 11904678]

Scheer S, Medina TS, Murison A, Taves MD, Antignano F, Chenery A, Soma KK, Perona-Wright G, Lupien M, Arrowsmith CH, et al. (2017). Early-life antibiotic treatment enhances the pathogenicity of CD4+ T cells during intestinal inflammation. J. Leukoc. Biol 101, 893–900. [PubMed: 28034915]

Scheinin T, Butler DM, Salway F, Scallon B, and Feldmann M (2003). Validation of the interleukin-10 knockout mouse model of colitis: antitumour necrosis factor-antibodies suppress the progression of colitis. Clin. Exp. Immunol 133, 38–43. [PubMed: 12823276]

Schildkraut V, Alex G, Cameron DJ, Hardikar W, Lipschitz B, Oliver MR, Simpson DM, and Catto-Smith AG (2013). Sixty-year study of incidence of childhood ulcerative colitis finds eleven-fold increase beginning in 1990s. Inflamm. Bowel Dis 19, 1–6. [PubMed: 22532319]

Schloss PD, Westcott SL, Ryabin T, Hall JR, Hartmann M, Hollister EB, Lesniewski RA, Oakley BB, Parks DH, Robinson CJ, et al. (2009). Introducing mothur: open-source, platform-independent, community-supported software for describing and comparing microbial communities. Appl. Environ. Microbiol 75, 7537–7541. [PubMed: 19801464]

Schreiber S, Khaliq-Kareemi M, Lawrance IC, Thomsen OO, Hanauer SB, McColm J, Bloomfield R, and Sandborn WJ; PRECISE 2 Study Investigators (2007). Maintenance therapy with certolizumab pegol for Crohn's disease. N. Engl. J. Med 357, 239–250. [PubMed: 17634459]

Segata N, Izard J, Waldron L, Gevers D, Miropolsky L, Garrett WS, and Huttenhower C (2011). Metagenomic biomarker discovery and explanation. Genome Biol. 12, R60. [PubMed: 21702898]

Singh V, Kumar M, San Yeoh B, Xiao X, Saha P, Kennett MJ, and Vijay-Kumar M (2016). Inhibition of interleukin-10 signaling induces microbiotadependent chronic colitis in apolipoprotein E deficient mice. Inflamm. Bowel Dis 22, 841–852. [PubMed: 26891260]

Surana NK, and Kasper DL (2017). Moving beyond microbiome-wide associations to causal microbe identification. Nature 552, 244–247. [PubMed: 29211710]

Tegtmeyer D, Seidl M, Gerner P, Baumann U, and Klemann C (2017). Inflammatory bowel disease caused by primary immunodeficiencies−clinical presentations, review of literature, and proposal of a rational diagnostic algorithm. Pediatr. Allergy Immunol 28, 412–429. [PubMed: 28513998]

Toussirot É, Houvenagel É, Goëb V, Fouache D, Martin A, Le Dantec P, Dernis E, Wendling D, Ansemant T, Berthelot JM, et al.; Le CRI (2012). Development of inflammatory bowel disease during anti-TNF-α therapy for inflammatory rheumatic disease: a nationwide series. Joint Bone Spine 79, 457–463. [PubMed: 22088934]

Üsküdar Cansu D, Üsküdar Teke H, Temel T, Ertürk A, Kahraman O, and Korkmaz C (2019). Do anti-TNF agents increase the risk of inflammatory bowel disease evolution in patients with ankylosing spondylitis? real life data. J. Natl. Med. Assoc 111, 262–269. [PubMed: 30389147]

Vital M, Howe AC, and Tiedje JM (2014). Revealing the bacterial butyrate synthesis pathways by analyzing (meta)genomic data. MBio 5, e00889. [PubMed: 24757212]

Walthall K, Cappon GD, Hurtt ME, and Zoetis T (2005). Postnatal development of the gastrointestinal system: a species comparison. Birth Defects Res. B Dev. Reprod. Toxicol 74, 132–156. [PubMed: 15834902]

Wang K, Han G, Dou Y, Wang Y, Liu G, Wang R, Xiao H, Li X, Hou C, Shen B, et al. (2012). Opposite role of tumor necrosis factor receptors in dextran sulfate sodium-induced colitis in mice. PLoS ONE 7, e52924. [PubMed: 23285227]

Wang Y, Han G, Chen Y, Wang K, Liu G, Wang R, Xiao H, Li X, Hou C, Shen B, et al. (2013). Protective role of tumor necrosis factor (TNF) receptors in chronic intestinal inflammation: TNFR1 ablation boosts systemic inflammatory response. Lab. Invest 93, 1024–1035. [PubMed: 23897411]

Waschke KA, Villani AC, Vermeire S, Dufresne L, Chen TC, Bitton A, Cohen A, Thomson AB, and Wild GE (2005). Tumor necrosis factor receptor gene polymorphisms in Crohn's disease: association with clinical phenotypes. Am. J. Gastroenterol 100, 1126–1133. [PubMed: 15842589]

Yu YR, O'Koren EG, Hotten DF, Kan MJ, Kopin D, Nelson ER, Que L, and Gunn MD (2016). A protocol for the comprehensive flow cytometric analysis of immune cells in normal and inflamed murine non-lymphoid tissues. PLoS ONE 11, e0150606. [PubMed: 26938654]

Zhang Y, Dubé PE, Washington MK, Yan F, and Polk DB (2012). ErbB2 and ErbB3 regulate recovery from dextran sulfate sodium-induced colitis by promoting mouse colon epithelial cell survival. Lab. Invest 92, 437–450. [PubMed: 22157714]

Highlights

- *Il10*$^{-/-}$ *Tnfr1*$^{-/-}$ mice exhibit severe colitis beginning shortly after weaning
- Colitis is dependent on the microbiome but is not taxa specific
- *Tnfr1*$^{-/-}$ mice exhibit colonic immune dysregulation and abnormal epithelium
- *Tnfr1*$^{-/-}$ mice have reduced cytokine expression during a critical weaning period

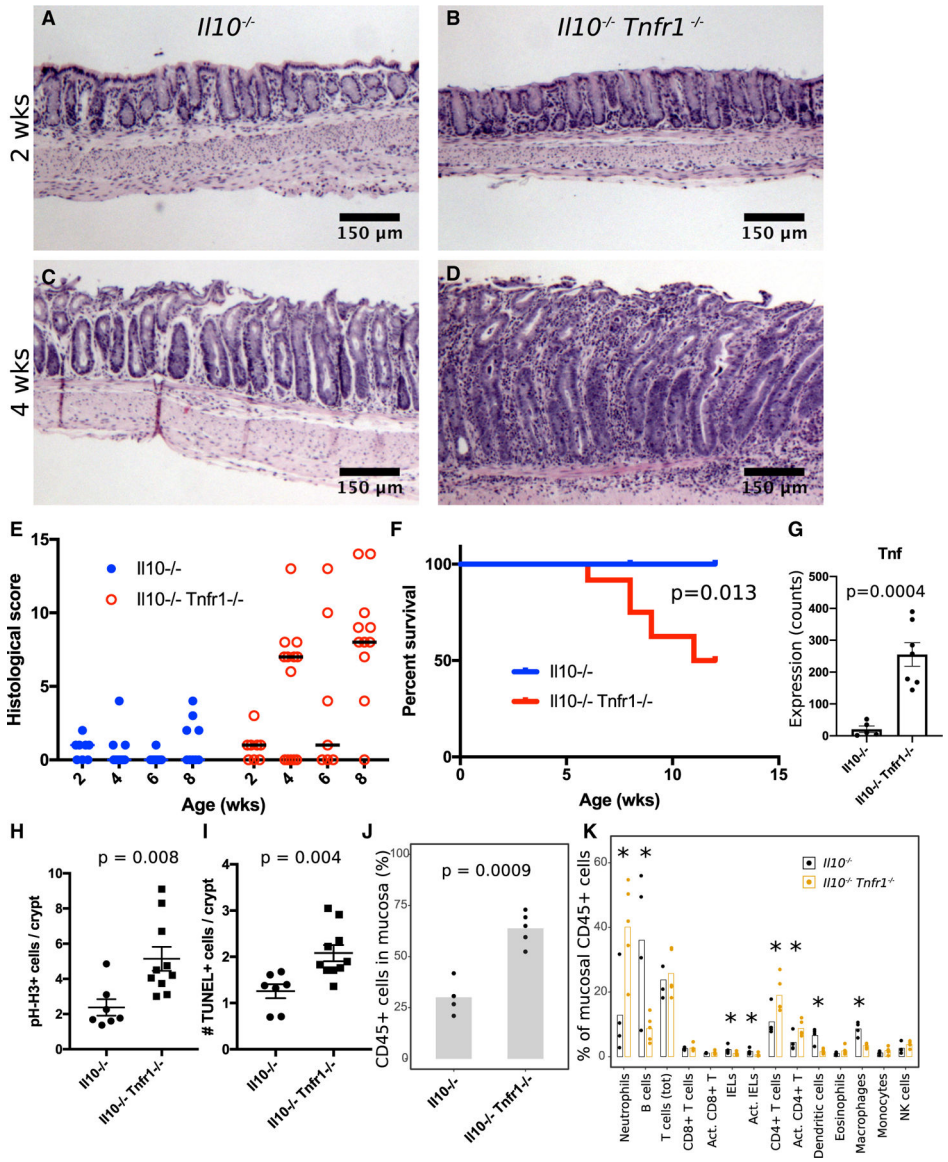

Figure 1. *Il10*$^{-/-}$ *Tnfr1*$^{-/-}$ Mice Develop Early-Onset, Severe Colitis at 4 Weeks Old

(A and B) Hematoxylin-and-eosin (H&E)-stained sections of pre-weaning 2-wk-old *Il10*$^{-/-}$ (A) (n = 7) and *Il10*$^{-/-}$ *Tnfr1*$^{-/-}$ (B) (n = 8) mice show normal distal colon.

(C and D) H&E sections of 4-week-old post-weaning mice reveal normal colon in the *Il10*$^{-/-}$ genotype (C) (n = 6) but colitis in the *Il10*$^{-/-}$ *Tnfr1*$^{-/-}$ genotype (D) (n = 13).

(E) Histological scoring of colitis severity (worst disease score is 15). Horizontal lines indicate median.

(F) Kaplan-Meier survival curve indicates early mortality in *Il10*$^{-/-}$ *Tnfr1*$^{-/-}$ mice.

(G) Nanostring analysis demonstrates upregulation of *Tnf* expression in *Il10*$^{-/-}$ *Tnfr1*$^{-/-}$ animals.

(H and I) Crypts in 12-wk-old *Il10*$^{-/-}$ *Tnfr1*$^{-/-}$ mice exhibited increased numbers of proliferating (pH-H3^{+}) (H) and apoptotic (TUNEL^{+}) (I) cells.

(J and K) Flow cytometric analysis of colonic mucosal scrapings demonstrates increased colonic mucosal infiltration of $CD45^+$ hematopoietic cells (J) with increased immune cell subsets (K) in 8-wk-old *Il10*$^{-/-}$ *Tnfr1*$^{-/-}$ mice.

Scale bars: (A)–(D) 100 μm. *$p < 0.05$. See also Figures S1, S2, and S3. Error bars: standard error.

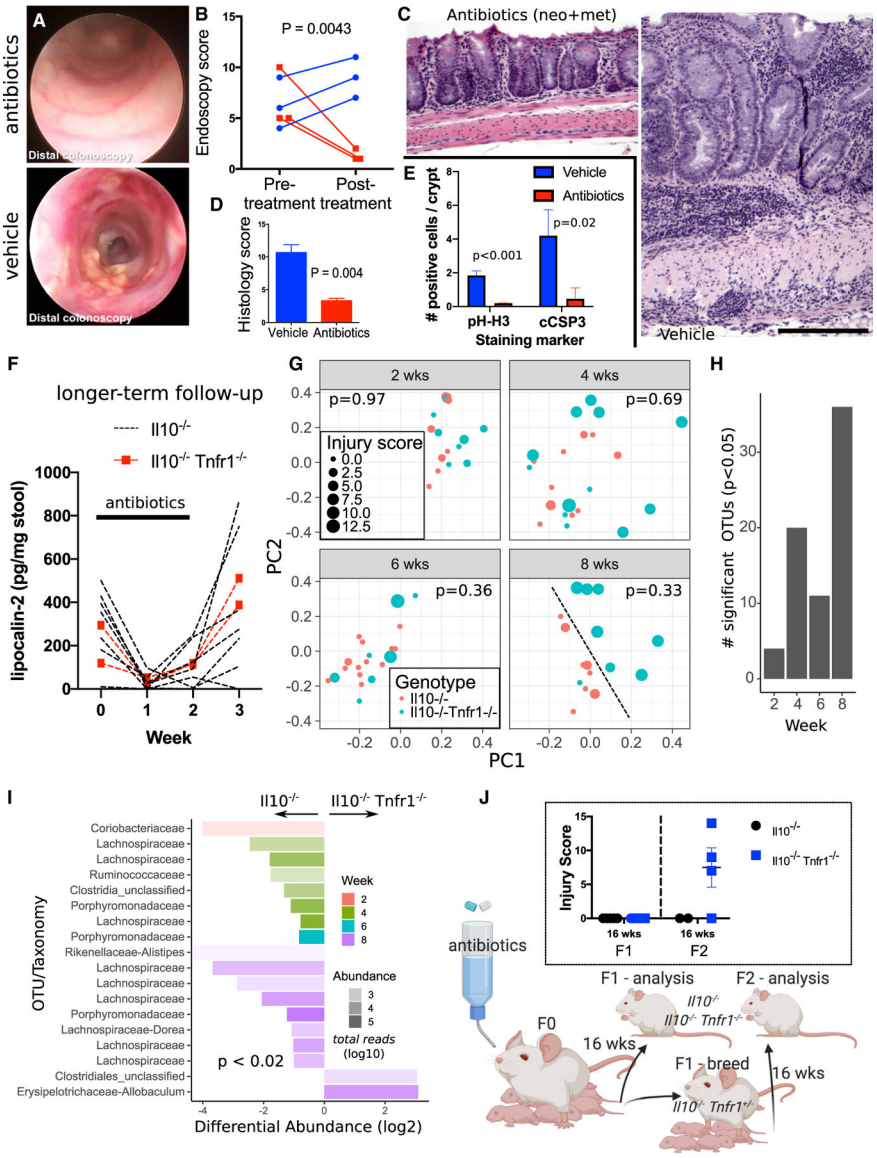

Figure 2. Broad-Spectrum Antibiotic Treatment Improves Colitis in *Il10*$^{-/-}$ *Tnfr1*$^{-/-}$ Mice

(A–E) Improved endoscopic appearance (A), endoscopic score (B), histology (C and D), and crypt cell dynamics (E) were observed in 8-week-old antibiotic-treated *Il10*$^{-/-}$ *Tnfr1*$^{-/-}$ mice (n = 3) compared with controls (n = 3).

(F) Fecal lipocalin levels diminished to nearly undetectable levels during antibiotic treatment of *Il10*$^{-/-}$ (n = 7) and *Il10*$^{-/-}$ *Tnfr1*$^{-/-}$ (n = 2) mice but quickly rebounded.

(G) 16S analysis of *Il10*$^{-/-}$ *Tnfr1*$^{-/-}$ and *Il10*$^{-/-}$ cecal microbiomes collected from 2-, 4-, 6-, and 8-week-old *Il10*$^{-/-}$ *Tnfr1*$^{-/-}$ and *Il10*$^{-/-}$ mice. Shown are weighted UniFrac distances plotted using multidimensional scaling. Each sample is coded by age (gray facets), genotype (color), and colitis score (size). At 8 weeks old, the genotypes could be qualitatively discriminated (dotted black line). The displayed p value for each age is computed by permuted analysis of variance using littermates, colitis severity, sex, and genotype conditioned on dam identity as model factors.

(H) Bar graph displays the total number of significant operational taxonomic units (OTUs) that are differentially abundant in *Il10*$^{-/-}$ versus *Il10*$^{-/-}$ *Tnfr1*$^{-/-}$ animals by age.
(I) OTUs with taxonomic classifications plotted to indicate their relative abundance in *Il10*$^{-/-}$ *Tnfr1*$^{-/-}$ versus *Il10*$^{-/-}$ samples. The transparency of the bars denotes the total abundance of the OTUs on a log scale (more transparent is less abundant).
(J) Depiction of the multigenerational experiment analyzing the effects of maternal antibiotic treatment on colitis development, with associated colitis scoring shown in the inset.
Scale bars: 200 μm. Error bars: standard error.

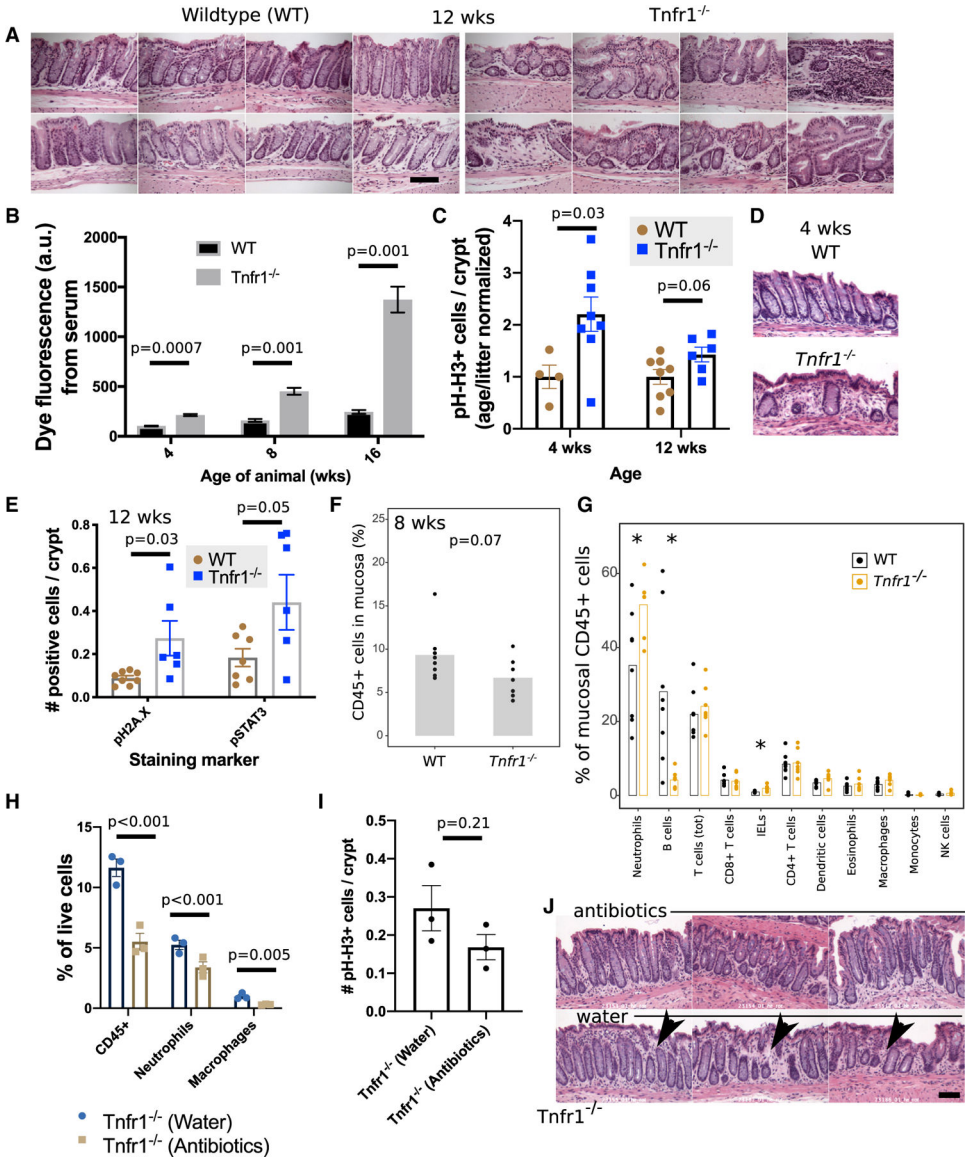

Figure 3. Adult *Tnfr1*$^{-/-}$ Mice Exhibit Epithelial Dysfunction and Alterations in Colonic Mucosal Immune Cell Representation

(A) Image montages show normal crypt structures in wild-type mice (n = 8) and focal abnormalities in 8-wk-old *Tnfr1*$^{-/-}$ mice (n = 7).

(B) *Tnfr1*$^{-/-}$ mice at 4, 8, and 12 weeks old exhibited increased colonic permeability at 30 min after rectal instillation of 4 kDa FITC-dextran. The graph is representative of three different experiments.

(C) Trending increase in pH-H3^{+} proliferative cells in knockout mice at 4 and 12 weeks old.

(D) H&E images of the colonic mucosa at 4 weeks old demonstrate foci of altered crypt patterning in *Tnfr1*$^{-/-}$ mice.

(E) Adult 12-week-old *Tnfr1*$^{-/-}$ colonic epithelium also had increased numbers of pH2A.X^{+} and pSTAT3^{+} cells.

(F and G) Flow cytometry reveals a trend toward decreased hematopoietic cell numbers (F) in the colonic mucosa of 8-week-old *Tnfr1*$^{-/-}$ mice. This was driven by increased neutrophils and a near-total loss of B cells (G).

(H) Flow cytometric assessment of antibiotic-treated *Tnfr1*$^{-/-}$ mice reveals reduced numbers of mucosal immune cells.

(I) Changes to pH-H3 staining after antibiotic treatment were more modest and insignificant.

(J) Qualitative reductions (arrowheads) in the density of inter-crypt cells were noted in H&E-stained sections of antibiotic-treated samples.

Scale bars: (A) 100 μm; (D) and (J) 50 μm, *$p < 0.05$. Error bars: standard error.

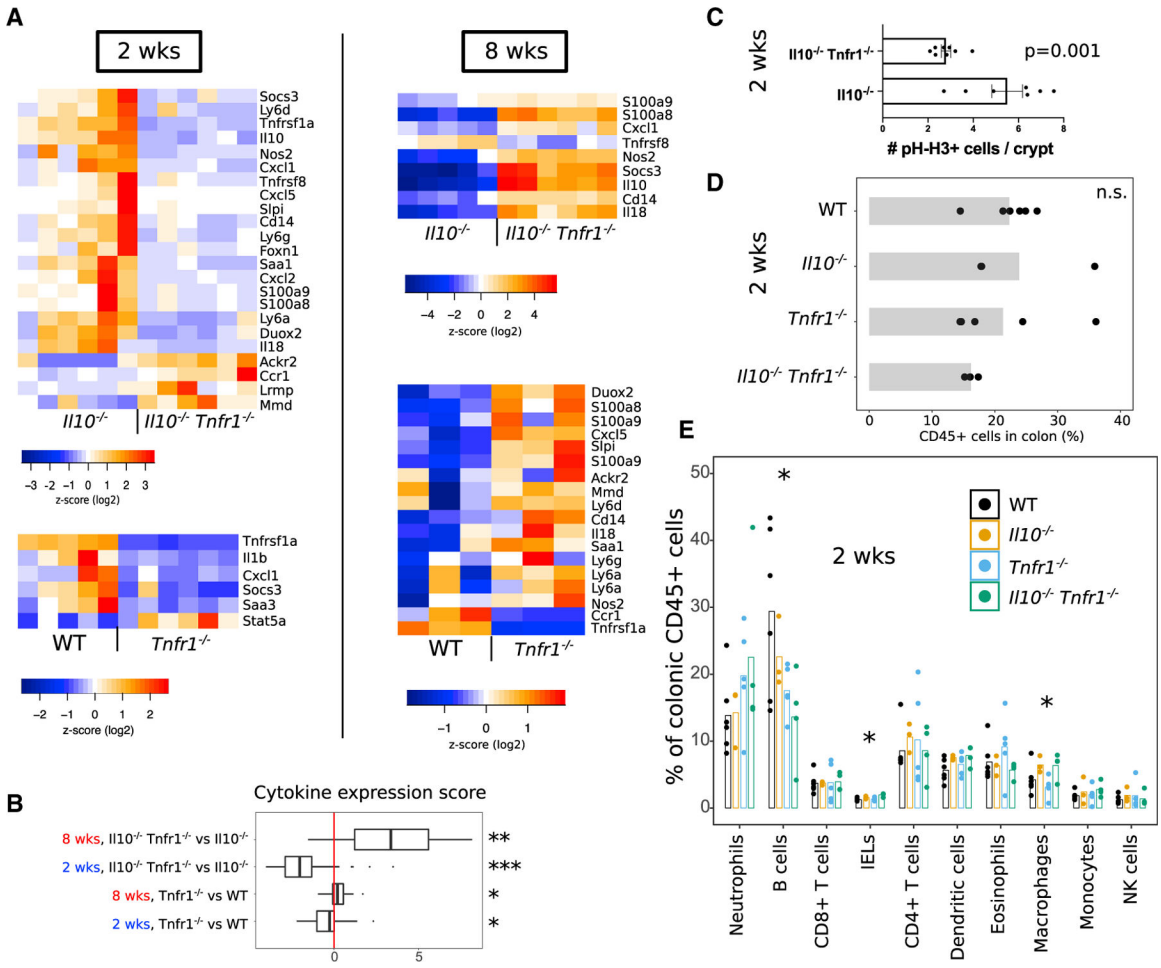

Figure 4. TNFR1-Deficient Animals Show Early-Life Defects in Colonic Immune Response

(A) Heatmaps summarize cytokine-expression levels obtained from RNA-seq/NanoString analysis of colons from wild-type (WT), *Tnfr1*$^{-/-}$, *Il10*$^{-/-}$, and *Il10*$^{-/-}$ *Tnfr1*$^{-/-}$ animals at 2 weeks (pre-disease) and 8 weeks (post-disease onset) old. Overall cytokine expression was decreased in TNFR1-deficient animals at 2 weeks of age but increased in those animals at 8 weeks old. Note that reads for *Il10* were still detected in *Il10*$^{-/-}$ animals because of continued production of mRNA encoding of an early-termination codon.

(B) The boxplot shows a summarized score of cytokine expression changes across comparisons of genotypes and ages. The lower and upper hinges represent the 25th and 75th percentiles. Whiskers denote the range of the data, excepting outlying points beyond 150% of the interquartile range. All values were obtained from RNA-seq except for the comparison of *Il10*$^{-/-}$ *Tnfr1*$^{-/-}$ versus *Il10*$^{-/-}$ mice at 8 weeks old (NanoString). Significance of scores was tested using the t test against 0 (no change).

(C) *Il10*$^{-/-}$ *Tnfr1*$^{-/-}$ animals at 2 weeks old show reduced pH-H3^{+} cell counts per crypt.

(D and E) Flow cytometric analysis of whole colons collected from 2-week-old mice shows overall similarity of colonic hematopoietic (CD45^{+}) cell counts (D) but loss of B cells in TNFR1-deficient animals (E).

Significance was evaluated using ANOVA. *p < 0.05. See also Figure S4. Error bars: standard error.

KEY RESOURCES TABLE

REAGENT or RESOURCE	SOURCE	IDENTIFIER
Antibodies		
FITC rat anti-CD45	Biolegend	103107; RRID: AB_312972
Alexa Fluor 700 rat anti-Ly6G	BD Biosciences	561236; RRID: AB_10611860
APC-Cy7 rat anti-CD11b	BD Biosciences	561039; RRID: AB_2033993
APC hamster anti-CD11c	BD Biosciences	561119; RRID: AB_10562405
PE rat anti-IA/IE	BD Biosciences	562010; RRID: AB_10893194
PE-Cy7 mouse anti-CD64	Biolegend	139313; RRID: AB_2563903
BV421 rat anti-CD24	BD Biosciences	562563; RRID: AB_2737002
PerCP-Cy5.5 rat anti-Ly6C	ThermoFisher Scientific	45-5932-80; RRID: AB_2723342
BV786 hamster anti-CD69	BD Biosciences	564683; RRID: AB_2738890
BV510 rat anti-CD8a	Biolegend	100751; RRID: AB_2561389
BV605 rat anti-CD4	Biolegend	100451; RRID: AB_2564591
PE-CF594 hamster anti-gdTCR	BD Biosciences	563532; RRID: AB_2661844
BUV395 hamster anti-CD3ε	BD Biosciences	563565; RRID: AB_2738278
Rabbit anti-pH2A.X (Ser139)	Cell Signaling Technology	9718S; RRID: AB_2118009
Rabbit anti-pH-H3 (Ser10)	Cell Signaling Technology	9701S; RRID: AB_331535
Rabbit anti-pSTAT3 (Tyr705)	Cell Signaling Technology	9145; RRID: AB_2491009
Rabbit anti-cleaved CSP3	Cell Signaling Technology	9661S; RRID: AB_2341188
truStain fcX (rat anti-CD16/32)	Biolegend	101320; RRID: AB_1574975
Rat anti-mouse IL-10R (CD210), 1B1.3A	Bio X Cell	BE0050; RRID: AB_1107611
Chemicals, Peptides, and Recombinant Proteins		
Neomycin sulfate – 500 mg tablets	Hi-Tech Pharmacal	50383-565-10
Metronidazole – 500 mg/100 mL	Claris Lifesciences	36000-001-24
4 kDa FITC-dextran	ThermoFisher Scientific	D3305
Liberase TM	Sigma-Aldrich	5401119001
DNase I	Sigma-Aldrich	D5025
Ultracomp eBeads	ThermoFisher Scientific	01-2222-41
Critical Commercial Assays		
16S library preparation	MR DNA (Molecular Research)	bTEFAP
mRNA-Seq library preparation (Illumina)	SeqMatic	20020594
nCounter Mouse Immunology Panel	Nanostring	XT-CSO-MIM1-12
Mouse Lipocalin-2/NGAL DuoSet ELISA	R&D Systems	DY1857
Deposited Data		
RNA-Seq (*Tnfr1*$^{-/-}$ versus WT, 8 wks of age)	Gene Expression Omnibus (GEO)	GSE107933
RNA-Seq (*Tnfr1*$^{-/-}$ versus WT, 2 wks of age)	Gene Expression Omnibus (GEO)	GSE155654
RNA-Seq (*Il10*$^{-/-}$ *Tnfr1*$^{-/-}$ versus *Il10*$^{-/-}$, 2 wks of age)	Gene Expression Omnibus (GEO)	GSE155626

REAGENT or RESOURCE	SOURCE	IDENTIFIER
Experimental Models: Organisms/Strains		
Mice: C57Bl6/J	Jackson Labs	000664
Mice: *Il10*$^{-/-}$	Jackson Labs	002251
Mice: *Tnfr1*$^{-/-}$	Jackson Labs	002818
Software and Algorithms		
Kallisto/sleuth v0.44.0	Pachter Lab	https://pachterlab.github.io/kallisto/
nSolver v3.0	Nanostring	https://www.nanostring.com/products/analysis-software/nsolver
mothur v1.40.1	Schloss Lab	https://mothur.org/
FlowJo v10.4	FlowJo	https://www.flowjo.com/